a forward model comparison will help us resolve any gradients of the magnetic field within the Hα line-forming heights.

We have seen the clarity of the inverse or reverse penumbral Evershed effect in the chromosphere, when compared to the photosphere. This clarity is not necessarily visible through all the penumbra, but only in small segments. Perhaps the complicated sunspot we observed attests to this non-uniformity. Since the magnetic polarities observed in the chromosphere are similar to that in the photosphere, one must perhaps invoke a complicated set of mechanisms to understand the chromospheric Evershed effect in the penumbra, rather than a simple siphon flow model.

Acknowledgments. We are grateful to Bruce Lites, HAO for his encouragement and help in observing the Hα spectral line with the ASP, along-with the photospheric spectral lines. We sincerely appreciate David Elmore's efforts in the continued function of the ASP. We are indebted to Thomas Rimmele and the NSO/Adaptive Optics team for improved image quality at the Dunn Solar Telescope. We thank Doug Gilliam and Joe Elrod for their diligent and meticulous observational support. Jackie Diehl proofread this manuscript.

References

Balasubramaniam, K. S., Uitenbroek, H., Harvey, J. W. & Jones, H. 2002, American Astronomical Society Meeting 2002, #38.07

Balasubramaniam, K. S. 2002, ApJ, 565, 553

Cauzzi, G., Smaldone, L. A., Balasubramaniam, K. S. & Keil, S. L. 1993, Solar Phys. 146, 207

Elmore, D. F., Lites, B. W., Tomczyk, S., Skumanich, A., Dunn, R. B., Schuenke, J. A., Streander, K. V., Leach, T. W., Chambellan, C. W., Hull, H. K., & Lacey, L. B. 1992, in Proc. SPIE, 1746, 22

Jefferies, J.T. & Mickey, D.L. 1991, ApJ, 372, 694.

Jones, H. P. 1982, Solar Phys., 79, 279

Jones, H. P., & Giovanelli, R. G. 1982, Solar Phys., 79, 247

Jones, H. P., & Giovanelli, R. G. 1983, Solar Phys., 87, 37

Landi Degl'Innocenti, E. & Landi Degl'Innocenti, M. 1973, Solar Phys., 31, 299

Lites, B. 1996, Solar Phys., 163, 223

Metcalf, T. R. & , Leka, K. D. 2001, American Geophysical Union, Spring Meeting 2001, abstract #SP41B-07

Rees, D. E., & Semel, M. D. 1979, A&A, 74, 1

Sigwarth, M. 2001, ASP Conf. Ser. Vol. 236, Advanced Stokes Polarimetry, Theory, Observation and Instrumentation, (San Francisco: ASP)

Skumanich, A., Lites, B. W., Martinez Pillet, V., & Seagraves, P. 1997, ApJS, 110, 357

Socas-Navarro, H., Trujillo Bueno, & J. Ruiz Cobo, B. 2000, ApJ, 530, 977

Current Theoretical Models and High Resolution Solar Observations: Preparing for ATST
ASP Conference Series, Vol. 286, 2003
A. A. Pevtsov and H. Uitenbroek, eds.

Modeling the Fine Structure of a Sunspot Penumbra through the Inversion of Stokes Profiles

J.M. Borrero, A. Lagg, S.K. Solanki

Max-Planck Institut für Aeronomie, 37191, Katlenburg-Lindau, Germany

C. Frutiger

Institute of Astronomy, ETH-Zentrum, 8092, Zurich, Switzerland

M. Collados

Instituto de Astrofísica de Canarias, 38200, Vía Láctea, Tenerife, Spain

L.R. Bellot Rubio

Kiepenheuer-Institut für Sonnenphysik, Schöneckstr. 6, 79104, Freiburg, Germany

Abstract. We have implemented the uncombed magnetic field model for a sunspot penumbra proposed by Solanki & Montavon (1993) in the inversion code by Frutiger & Solanki (2000). The discontinuity along the line of sight, produced by the presence of one or more horizontal flux tubes embedded in a magnetic surrounding, is treated using the interlaced atmospheres approach by Del Toro Iniesta et al. The Response Functions for the embedded and inclined flux tubes are calculated numerically. We present the results of tests showing to what extent the inversion code is able to reproduce the properties of embedded flux tubes. A sample application to observed data is also briefly presented.

1. Introduction

Inversion codes have been repeatedly used to infer the thermodynamical properties of the penumbra in sunspots. Inversions based on 1 component models exhibit large gradients along the line-of-sight velocity and magnetic field inclination (see Sánchez Almeida & Lites 1992; Westendorp Plaza et al. 2001a, 2001b; Bellot Rubio et al. 2002). Such gradients are unlikely to be due to global properties of the sunspot (Solanki, Walther & Livingston 1993) but rather to its fine structure. Later inversions based on 2-component Models (see Del Toro Iniesta, Bellot Rubio & Collados 2001) reveal the existence of a penumbral model almost at rest and with a magnetic field that is significantly inclined to the horizontal and a second component with more horizontal velocity and magnetic field. This picture nicely fits with the model for the uncombed magnetic field proposed by Solanki & Montavon (1993) in which a horizontal flux tube is embedded in a

more vertical background. The next step will be to deal with the discontinuity along the line–of–sight produced by the presence of these flux tubes. To this end we have implemented the uncombed model in the inversion code from Frutiger & Solanki (2000). In order to be able to deal with such a discontinuity we use the strategy presented by Del Toro Iniesta et al. (1995). Here we present some details about the implementation of the uncombed model as well as some numerical tests to study its feasibility to retrieve the original atmosphere under simulated and real observations.

2. The Umcombed Model

The adopted model describing the uncombed magnetic field can be considered as a 2-component model. The first component is a pure penumbral background while the second also includes such a background but with a horizonzal flux tube embedded at a certain geometrical depth z_0 and with a given diameter D_{tube} (see Figure 1 upper panel). In the following, index (t) corresponds to flux tube component and (s) is for the surrounding atmosphere. From force balance considerations we impose the following constraints:

- The background component is considered to satisfy vertical hydrostatic equilibrium neglecting the magnetic tension and the radiation pressure:[1]

$$P_{g,s}(z) = P_{g,s}(z_0)\exp\left[-\frac{g}{m_H K_B}\int_{z_0}^{z}\frac{\mu_s(z')}{T_s(z')}dz'\right] \quad (1)$$

- The gas pressure inside the tube is obtained from horizontal equlibrium between both components:

$$P_{g,t}(z) = P_{g,s}(z) + \frac{B_s^2(z) - B_t^2(z)}{8\pi} \quad (2)$$

Since the properties of this flux tube can be very different from the background (see Figure 1 bottom panel) we obtain the needed discontinuities along the line of sight to produce a net circular polarization: see Solanki & Montavon (1993) and its center to limb variation (Martínez Pillet 2000). The total emergent intensity is obtained after the intensity coming from the flux tube component is added (through a filling factor: α_T) to the intensity produced by the purely penumbral background model. Finally, it must be pointed out that, since we sample the whole unresolved structure with only two rays at a given cut on the $x = x_0$ (where $\hat{e_x}$ is the vector parallel to the tube axis, see top panel on Figure 1), we can only deal with rather horizontal (with respect to the normal vector on the solar surface: $\hat{e}_z$) flux tubes. Under this assumption the definition of Z_0 makes sense and its value is unique within a pixel[2].

[1] Where P_g is the gas pressure, the solar surface gravity $g = 2.74\,10^4\ cm\ s^{-2}$, m_H is the proton mass, K_B is the Boltzmann's constant, μ the mean molecular weight, T is the temperature and z_0 is the geometrical height on the top of the atmosphere.

[2] Under this assumption, for a cut in a plane $x = x_k \neq x_0$ (See Figure 1, top panel) the value for Z_0 will be the same

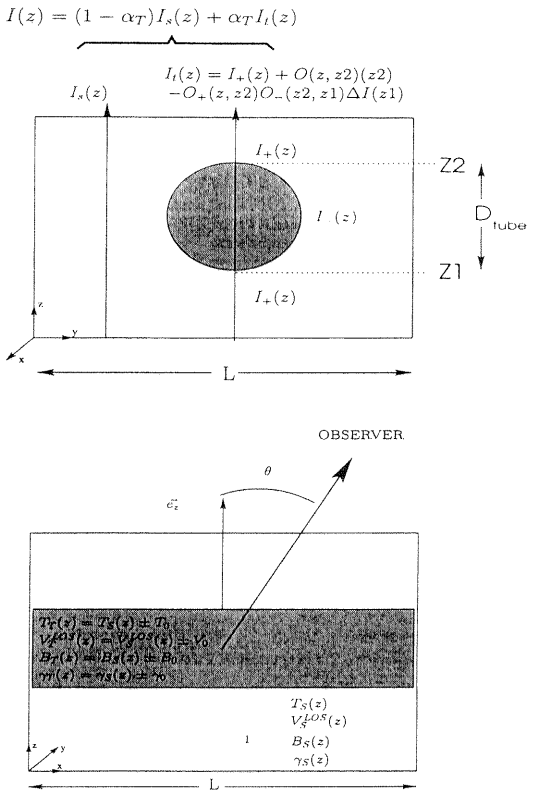

Figure 1. Schematics of the geometry of a horizontal flux tube. Top panel: cut in the plane $x = x_0$ perpendicular to the tube axis. Two single rays allow us to sample the structure; rays passing at a different distance from the flux tube center are treated using the approach of Del Toro Iniesta et al. (1995) for interlaced atmospheres (see also Frutiger 2001). Bottom panel: the thermodynamic, magnetic and dynamic properties of the flux tube are obtained after adding a constant value on the surrounding atmosphere's stratifications.

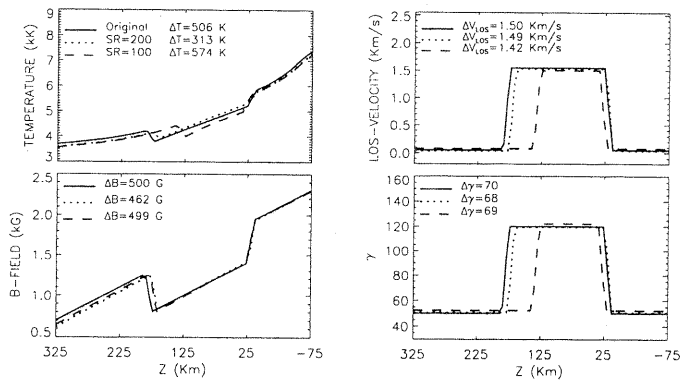

Figure 2. Atmospheres resulting from the inversion (with the uncombed model) of the noisy Stokes profiles synthesized with the original atmosphere (solid curves) containing a horizontal flux tube: $\gamma = 120^o$ and $\alpha_T = 0.35$. Dotted curves: SN^{-1} =200 in Stokes I; Dashed curves: the same but SN^{-1} =100.

3. Test A: Horizontal Tubes

To test the behaviour of the implementation and its ability to retrieve the atmospheric parameters through the inversion of spectral lines, we have synthesized two spectral lines of neutral iron in the infrared: Fe I 15648 Å and 15652 Å . They were synthesized using an horizontal flux tube ($\gamma = 120^o$, $\alpha = 0.35$, $\theta = 25^o$). To simulate real observations we have added noise to the synthetic profiles at different levels (SN^{-1}=200,100) in units of the continuum intensity (SN^{-1}=20,10 for polarized profiles). Then we invert these profiles using an initial guess model rather different from the real one. The results are shown in Figure 2 (recovered atmospheres), Figure 3 (best fit profiles) and Table 1 (tube parameters).

4. Test B: Atmosphere with no Tube

Another test we have carried out concerns the ability of the code to distinguish between an atmosphere (through the inversion of its emergent spectra) which contains a flux tube from another which does not. This is important since not all the stokes profiles at each pixel in the penumbra need atmospheres with large gradients along the line of sight to be properly reproduced, suggesting perhaps that there is no flux tube in them or that it has a rather insignificant contribution. We have therefore computed a synthetic spectra using a 1-component magnetic atmosphere, and after adding noise (again at levels so that a SN^{-1} of 200,100 is achieved in the continuum) we have inverted the profiles using the uncombed model with an initial tube whose filling factor $\alpha_T = 0.35$. In principle

Table 1. Test A: Parameters for the horizontal flux tube used to synthesize the line profiles (top row) and retrieved parameters after adding several noise levels to the synthetic profiles (2nd and 3rd rows). We have used the same initial guess model for both inversions. It turns out that the real atmosphere is recovered showing the robustness of the code when a horizontal flux tube is present.

SN^{-1}	α_T	$Z_0(km)$	$D_{tube}(km)$	$\Delta T(K)$	$\Delta V_{LOS}(km/s)$	$\Delta B(G)$	$\Delta\gamma$
Real	0.35	100	150	500	1.50	500	70
200	0.36	84	143	313	1.49	462	68
100	0.39	80	93	574	1.42	499	69

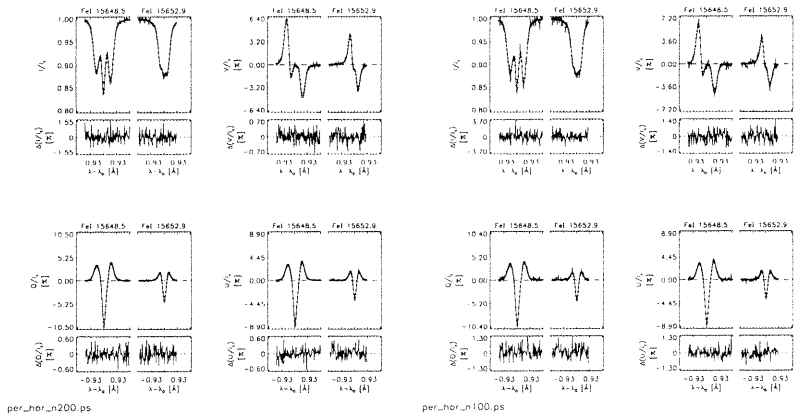

Figure 3. Best fit profiles to the noisy synthetic Stokes spectra. Left panels: SN^{-1}=200 and right Panels: SN^{-1} = 100. Note that when the profiles are very degraded (right panel) the fingerprints of the flux tube on the profiles are masked by the noise so that the real atmosphere is not completely recovered (Figure 2 and Table 1).

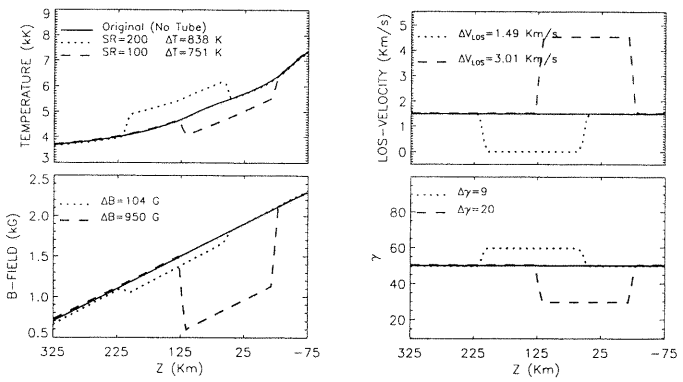

Figure 4. Inferred atmospheres from the inversion of noisy profiles synthesized (dashed: SN^{-1}=100, dotted: SN^{-1}=200) using a one component model without tube (solid).

there are two ways in which the code can tell us that it finds no flux tube in the profiles: either setting $\alpha_T = 0$ or returning a tube whose thermodynamic, magnetic and dynamic properties are identical to the surroundings. After performing the inversions we see that the code tends to diminish α_T to tiny values (Table 2) while the properties of the flux tube (Figure 4) are still rather different from the real atmosphere. However it turns out that the atmosphere surrounding the tube is almost identical to that used in the synthesis (and since the filling factor of the tube is very small, its contribution to the final spectrum is minimal).

5. Application to Real Observations

As an example we present the result for one pixel in a sunspot of the active region AR 8704 at an heliocentric angle of $\theta = 24$ ($\mu = 0.91$). Spectropolarimetric data of the two infrared lines at 1.56μm was recorded using the Tenerife Infrared Polarimeter (TIP) attached to the VTT (Vacuum Tower Telescope) at Izaña Observatory (see Schlichenmaier & Collados 2002). This pixel is just before the apparent neutral line on the limb side of the sunspot and shows an extremely unusual V profile which seems to be suitable to apply the uncombed model. The signal to noise ratios for this pixel is about 250 for I and 50 for Q, U and V. According to the test already performed we expect (under the assumption that our model for the penumbra is realistic) to recover the real atmosphere. The best fit profiles are shown in Figure 5, while the retrieved atmosphere is in Figure 6. Except for the discrepancy at the central lobe of the V profile for Fe I 15648, the fit is very satisfactory, supporting the reliability of the uncombed model.

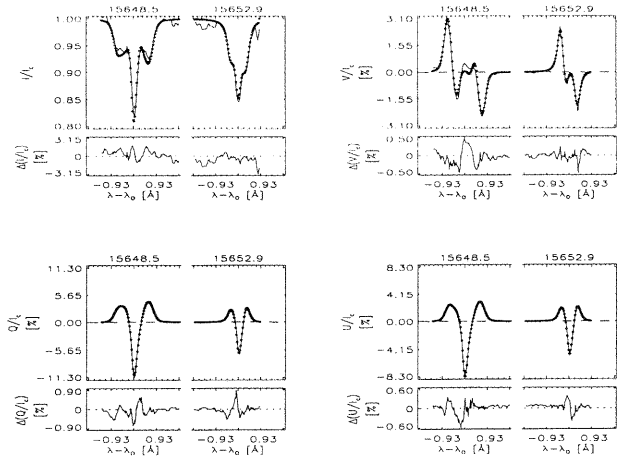

Figure 5. Best fit profiles for a pixel at the inner limb side penumbra in a sunspot. The poor fit in the wings of 15652 Å is due to molecular blends and interference bands in the observations.

Table 2. Inferred filling factors of the tube when inverting profiles previously synthesized using an atmosphere with no tube: Test B.

SN^{-1}	Real	200	100
α_T	0.00	0.01	0.03

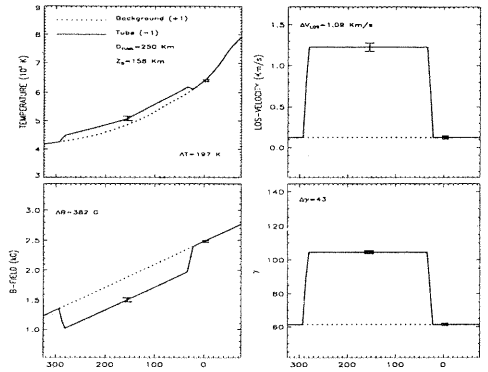

Figure 6. Properties of the flux tube retrieved from fits to the spectral lines on Figure 5. The flux tube shows an internal velocity inclined 81 degrees in the local reference frame (almost horizontal) and an absolute velocity of 4.7 kms^{-1}. It is (given the error bars) slightly hotter than the surroundings and possesses a much smaller magnetic field. If we trust these results: would this correspond to an observational feature of a later evolution stage from one of Schlichenmaier et al.'s(1998) rising flux tubes?

References

Bellot Rubio, L.R., Collados, M., Ruis Cobo, B., & Rodríguez Hidalgo, I. 2002, Il Nuovo Cimento (in press)

Del Toro Iniesta, J.C., Ruiz Cobo, B., Bellot Rubio, L.R. & Collados, M. 1995, A&A, 294, 855

Del Toro iniesta, J.C., Bellot Rubio, L.R. & Collados, M. 2001, ApJ, 549, L139

Frutiger, C., Solanki, S.K., Fligge, M., & Bruls, J. 2000, Ap&SS, 243, 281

Frutiger, C., 2000, PhD thesis, Institute of Astronomy, ETH–Zurich

Martínez Pillet, V. 2000, A&A,361,359

Schlichenmaier, R.,Jahn, K., & Schmidt, H.U. 1998, A&A, 337, 897

Schlichenmaier, R., & Collados, M. 2002, A&A, 381, 668

Sánchez Almeida, J., & Lites, B. 1992, ApJ, 398, 359

Solanki, S.K., Montavon, C.A.P. 1993, A&A, 275, 283

Solanki, S.K., Walther, U., & Livingstone, W. 1993, ASP Conf. Ser, IAU Colloquium 141, 41

Westendorp Plaza, C., Del Toro Iniesta, J.C., Ruiz Cobo, B., Martínez Pillet, V., Lites, B. & Skumanich A. 2001, ApJ, 547, 1130

Westendorp Plaza, C., Del Toro Iniesta, J.C., Ruiz Cobo, B., Martínez Pillet, V., Lites, B. & Skumanich A. 2001, ApJ, 547, 1148

Current Theoretical Models and High Resolution Solar Observations: Preparing for ATST
ASP Conference Series, Vol. 286, 2003
A. A. Pevtsov and H. Uitenbroek, eds.

Statistical Properties of Asymmetries in and around Sunspots

K. Sankarasubramanian, T. Rimmele

National Solar Observatory/Sacramento Peak Observatory, Sunspot, NM 88349, USA

Abstract. We studied the statistical properties of V-profile asymmetries in and around several sunspots. The properties are clearly separated for different regions in the sunspot (like umbral region, penumbral region, light bridges, and small-scale fields surrounding the sunspot). Each of the sunspot showed a bi-model distribution in the scatter plot between area and amplitude asymmetry. The sunspot umbra showed very little area and amplitude asymmetries whereas the penumbral region showed larger area asymmetries compared to the amplitude asymmetries. The light bridges and small-scale fields showed larger amplitude asymmetries compared to the area asymmetries. The relation between the difference of the amplitude and area asymmetry with the velocity gradient showed a linear relation confirming that the asymmetries are produced by velocity gradients.

1. Introduction

V-profile asymmetries are interpreted as the effect of gradient or discontinuity in the velocity along the line-of-sight (LOS). A gradient or discontinuity in magnetic field can reduce or enhance the asymmetries (see e.g., Auer & Heasley 1978; Sanchez Almeida & Lites, 1992). These asymmetries were observed first by Illing, Landmann, & Mickey (1975). They observed a non-zero net circular polarization using a broad band filter (10nm bandwidth around 530nm). Measurements of the asymmetries using a single absorption line were done by several authors (see e.g., Sanchez Almeida & Lites 1992; Solanki, Rüedi, & Rabin 1993; Sanchez Almeida et al. 1996; Sigwarth et al. 1999; Sankarasubramanian 2000; Schlichenmaier & Collados 2001; Sankarasubramanian & Rimmele 2002). Now it is known that the V-profile asymmetries are present all over the sun and have been observed for different active regions like sunspot (Sanchez Almeida & Lites 1992), plages (Martinez Pillet, Lites, & Skumanich 1997), pores (Leka & Steiner 2001), and small-scale fields (Sigwarth et al. 1999). The strength of the asymmetry varies from mild to strong. In some cases, V-profile shows multiple reversal like for e.g. in the neutral line region (known as 'cross-over effect', Solanki, Rüedi, & Rabin 1993; Sanchez Almeida et al. 1996; Sigwarth et al. 1999; Sankarasubramanian 2000).

The observations by Sankarasubramanian & Rimmele (2002) using the low-order Adaptive Optics (AO) system and with the Advanced Stokes Polarimeter

A SERIES OF BOOKS ON RECENT DEVELOPMENTS IN
ASTRONOMY AND ASTROPHYSICS

Publisher

THE ASTRONOMICAL SOCIETY OF THE PACIFIC

390 Ashton Avenue, San Francisco, California, USA 94112-1722
Phone: (415) 337-1100 E-Mail: orders@astrosociety.org
Fax: (415) 337-5205 Web Site: www.astrosociety.org

ASP CONFERENCE SERIES - EDITORIAL STAFF
Managing Editor: D. H. McNamara
LaTeX-Computer Consultant: T. J. Mahoney (Spain) – tjm@ll.iac.es
Production Manager: Enid L. Livingston
Production Assistant: Andrea Weaver

PO Box 24453, Room 211 - KMB, Brigham Young University, Provo, Utah, 84602-4463
Phone: (801) 422-2111 Fax: (801) 422-0624 E-Mail: pasp@byu.edu

ASP CONFERENCE SERIES PUBLICATION COMMITTEE:
Joss Bland-Hawthorn
George Jacoby
James B. Kaler
J. Davy Kirkpatrick

A listing of all of the ASP Conference Series Volumes and IAU Volumes published by The ASP may be found at the back of this volume

ASTRONOMICAL SOCIETY OF THE PACIFIC
CONFERENCE SERIES

Volume 286

CURRENT THEORETICAL MODELS AND HIGH RESOLUTION SOLAR OBSERVATIONS: PREPARING FOR ATST

Proceedings of the 21st Sacramento Peak Workshop held at the
National Solar Observatory, Sacramento Peak, Sunspot, New Mexico, USA
11-15 March 2002

Edited by

Alexei A. Pevtsov
National Solar Observatory, Sacramento Peak, Sunspot, New Mexico, USA

and

Han Uitenbroek
National Solar Observatory, Sacramento Peak, Sunspot, New Mexico, USA